# Thermal Shock Fracture of Zirconia Ceramics

Tsugio Sato, Masayuki Ishitsuka, Tadashi Endo and Masahiko Shimada
Department of Molecular Chemistry and Engineering, Faculty of Engineering, Tohoku University, Aoba, Sendai 980, Japan
Haruo Arashi
Research Institute for Scientific Measurements, Tohoku University, Katahira, Sendai 980, Japan

## Abstract

Thermal shock fracture behaviour of various kinds of zirconia ceramics such as magnesia partially stabilized zirconia (Mg-PSZ), yttria and ceria-doped tetragonal zirconia polycrystals (Y-TZP and Ce-TZP), Y-TZP/$Al_2O_3$ composites and yttria-doped cubic stabilized zirconia (Y-CSZ) was evaluated together with that of alumina, mullite, silicon nitride and silicon carbide by quenching method using water, methyl alcohol and glycerin as quenching media. Thermal shock fracture of all ceramics was proceeded by the thermal stress due to convective heat transfer accompanied by boiling of solvents under the present experimental conditions. Thermal shock resistance of zirconia based ceramics increased with increasing the fracture strength, but that of Y-TZP and Y-TZP/$Al_2O_3$ composites was anormalously lower than the

predicted value, since the toughening mechanism of zirconia by the stress-induced phase tranformation did not sufficiently function against the thermal stress fracture of Y-TZP based ceramics.

## 1. Introduction

Since ceramic materials show excellent high temperature fracture stength and chemical stability, they have been leading candidates for high temperature structural applications. Thermal shock resistance of ceramic materials is one of the most important properties, because brittle ceramics are susceptible to catastrophic failure under conditions of thermal stress introduced by the temperature difference ( $\Delta T$). Many studies have been carried out to elucidate the basic principles governing the thermal stress fracture of brittle ceramics. The quenching test into liquid media such as water, silicon oil, etc. has been used extensively for characterizing the thermal shock resistance of ceramics [1-3]. It was reported [4] that the observed thermal shock resistance was generally in good agreement to the predicted value by the thermal shock resistance parameter expressed by equation (1).

$$R_o = \sigma_f(1-\nu)/\alpha E \qquad (1)$$

where $\sigma_f$ is the fracture strength, $\nu$ is Poisson's ratio, $\alpha$ is the linear thermal expansion coefficient and E is Young's modulus. Since zirconia based ceramics such as Y-TZP show extensively high fracture strength such as 800-2500 MPa [5,6] due to the transformation toughening mechanism, they are expected to show excellent thermal shock resistance. However, thermal shock resistance of zirconia based ceramics were modest [7-11] and the

details have not been clarified yet. In the present paper, the thermal stress fracture behaviour of zirconia based ceramics such as Y-TZP, Y-TZP/$Al_2O_3$ etc. was evaluated by quenching method in detail.

## 2. Experimental

Yttria doped tetragonal zirconia powders containing 2 and 3 mol% $Y_2O_3$ (2Y-TZP and 3Y-TZP), yttria doped cubic stabilized zirconia powder containing 6 mol% $Y_2O_3$ (6Y-CSZ), ceria doped tetragonal ziconia powders containg 8, 12 and 16 mol% $CeO_2$ (8Ce-TZP, 12Ce-TZP and 16Ce-TZP), and 2Y-TZP/$Al_2O_3$ powders containing 10, 20 and 40 wt% $Al_2O_3$ supplied by Toso Co. were used as starting materials. These powders were isostatically pressed at 200 MPa to form plates (5x30x50 mm) and sintered at 1500$^{o}$C for 3-10 hr in air. The sintered bodies of 2Y-TZP/$Al_2O_3$ were hot isostatically pressed at 1450$^{o}$C and 150 MPa for 1 hr in Ar gas atmosphere. The sintered body of mullite was fabricated by the procedures described in the previous paper [12]. The sintered bodies of Mg-PSZ, SiC and $Si_3N_4$ were supplied by Nilcra Ceramics PTY Ltd., NGK Spark Plug Co., Ltd. and Toshiba Co., respectively. The characteristics of the samples used are summarized in Table 1 [10]. The samples were cut into bars (5x2x15 mm) and polished to parallel mirror like plane. The thermal shock resistance of each specimen was determined by quenching test using water, methyl alcohol and glycerin at 0$^{o}$C as quenching media. The bending strength of the specimen was determined by 3-point bending test with a cross head speed of 0.5 mm/min and span length of 10 mm. The Raman spectra around the cracks introduced by the thermal stress were recorded using a double monochrometer and photon

Table 1. Characteristics of the Sintered Bodies [10]

| Material | $\alpha$ ($\times 10^{-6}$/K) | $\nu$ | E (GPa) | k (W/m·K) | $\sigma_{3b}$ (MPa) | $R_o$ |
|---|---|---|---|---|---|---|
| $Al_2O_3$ | 7.4 | 0.27 | 393 | 18.5 | 300 | 75 |
| SiC | 3.2 | 0.25 | 330 | 91 | 330 | 234 |
| $Si_3N_4$ | 3.2 | 0.25 | 330 | 25 | 500 | 355 |
| Mg-PSZ | 10.1 | 0.23 | 205 | 1.8 | 460 | 171 |
| 6Y-CSZ | 9.0 | 0.25 | 200 | 3.5 | 240 | 100 |
| 3Y-TZP | 9.0 | 0.25 | 200 | 3.5 | 900 | 292 |
| 2Y-TZP | 9.0 | 0.25 | 200 | 3.5 | 1300 | 542 |
| 2Y-TZP/10 vol% $Al_2O_3$ | 8.8 | 0.25 | 229 | 3.5* | 1720 | 640 |
| 2Y-TZP/20 vol% $Al_2O_3$ | 8.6 | 0.26 | 254 | 5.7* | 2060 | 698 |
| 2Y-TZP/40 vol% $Al_2O_3$ | 8.2 | 0.26 | 298 | 7.8* | 2070 | 627 |
| 8Ce-TZP | 5.2 | 0.25 | 200 | 3.5* | 600 | 433 |
| 12Ce-TZP | 10.9 | 0.25 | 200 | 3.5* | 425 | 146 |
| 16Ce-TZP | 5.8 | 0.25 | 200 | 3.5* | 160 | 103 |

$R_o = \sigma_{3b}(1-\nu)/\alpha E$ *:Estimated

counting system using 514.5 nm lines of Ar-ion laser as exciting lighl for the following optical conditions: probe diameter ca. 4 um, objective lens x40, spectrum scan rate 6 $cm^{-1}$/min and resolution power 2.5 $cm^{-1}$.

3. Results and Discussion

The thermal shock fracture tests of 3Y-TZP and $Al_2O_3$ were carried out using water, methyl alcohol and glycerin at $0^oC$ as quenching media. The relationship between the 3-point bending strength of quenched samples and the temperature difference between the samples and quenching media are shown in Figs. 1 and 2 [10]. A variety of the critical quenching temperature difference ( $\Delta T_c$) above which the fracture strength of the queched sample degrades such as 275-475$^oC$ for 3Y-TZP and 200-350$^oC$ for $Al_2O_3$ were observed by using different quenching media. These results indicated that the magnitude of the thermal stress greatly depended on the characteristics of the quenching media.

The thermal stress, $S_t$, introduced into the ceramic materials can be described by following equation.

$$S_t = \sigma^* \alpha E \Delta T/(1-\nu) \quad (2)$$

where $S_t$ is the tensilestress introdued into the sample at the temperature difference of $\Delta T$ and $\sigma^*$ is a nodimentional maximum thermal stress depending on the quenching conditions. Since $S_t$ equals the tensile strength, $\sigma_t$, of the materials at the critical quenching temperature difference, $\Delta T_c$, equation (3) can be deribed from eqation (2).

$$\Delta T_c = \sigma_t(1-\nu)/\sigma^* \alpha E \quad (3)$$

Two kinds of heat transfer mechanism, i.e., conductive heat transfer and convective heat transfer, have been considered to

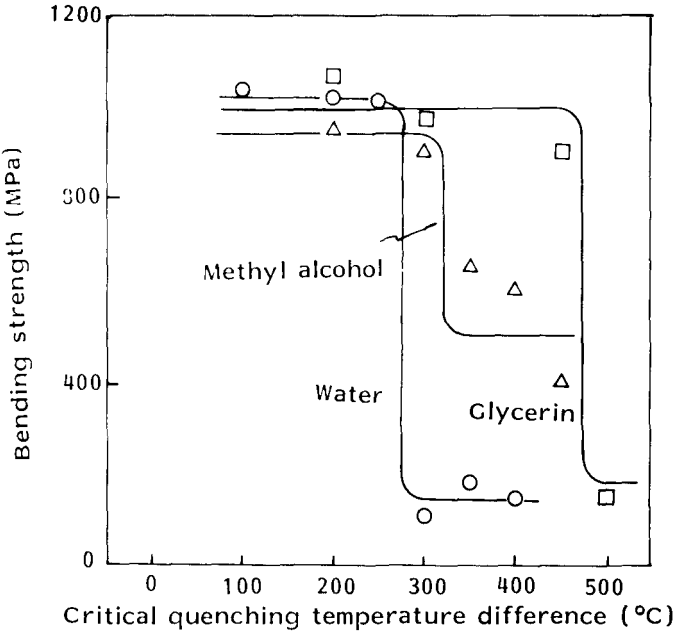


Fig. 1 Relation between 3-point bending strength of 3Y-TZP and quenching temperature difference for various quenching media [10].

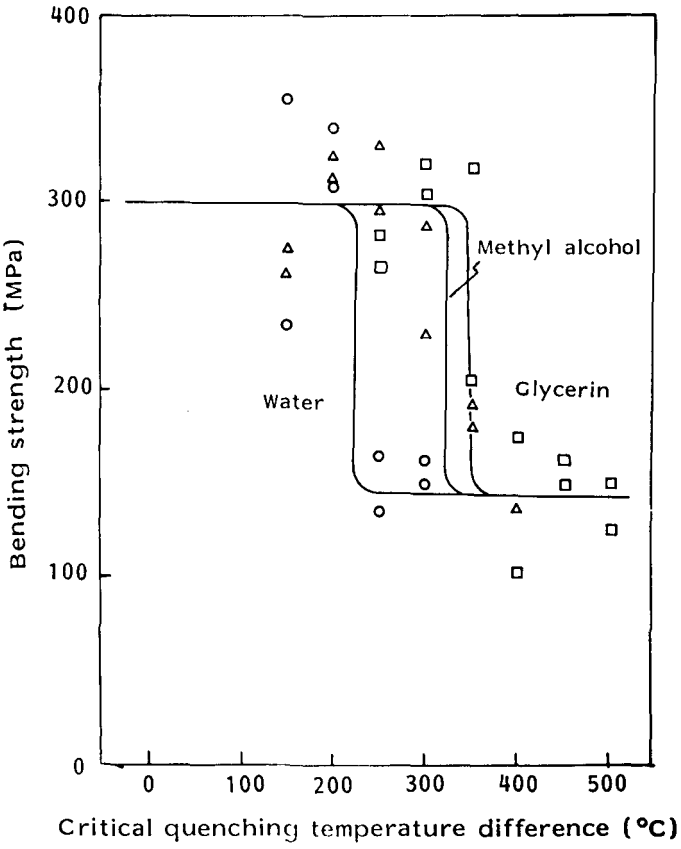


Fig. 2 Relation between 3-point bending strength of $Al_2O_3$ and quenching temperature difference for various quenching media [10].

interpret the experimental data for thermal shock resistance of ceramics obtained by the quenching test. $\sigma^*$ for convective heat transfer and conductive heat transfer mechanism can be expressed by equations (4) and (5), respectively [13,14].

$$1/\sigma_v^* = 1.451(1 + 3.42k_1/rh) \quad (4)$$

$$1/\sigma_d^* = (k_1\rho_1c_1/k_2\rho_2c_2)^{1/2} + 1 \quad (5)$$

where r is radius for cylinder sample and half thickness for plate sample, h is heat transfer coefficient, k is thermal conductivity, C is specific heat, $\rho$ is density and subscripts 1 and 2 refer to the specimen and quenching medium, respectively.

The nondimentional thermal stresses, $\sigma_v^*$ and $\sigma_d^*$ at the quenching test of 3Y-TZP and $Al_2O_3$ were calculated by equations (4) and (5) and listed in Table 2 [10] together with the thermophysical properties of each solvent, where h was calculated by Holman's equation (6) [15] by assuming natural convection.

$$h = 0.53(Gr \cdot Pr)^{1/4}(k_2/2r) \quad (6)$$

$$Gr = gB_2(T_1-T_2)(2r)^3\,\rho_2{}^2/\mu_2{}^2, \quad Pr = c_2\mu_2/k_2$$

where Gr and Pr are Grashof number and Prandtl number, respectively, g is the gravitational constant, B is the volumetric thermal expansion coefficient and $\mu$ is the viscosity. The quantity $(T_1-T_2)$ was taken to be $300^oC$ for all calculations. As seen in Table 2, for all quenching media, $\sigma_d^*$ was greater than $\sigma_v^*$. Therefore, it was suspected that the conductive heat transfer caused greater thermal stress than convective heat transfer caused by natural convection. The relationship between $\Delta T_c$ and $1/\sigma_d^*$ for 3Y-TZP and $Al_2O_3$ is shown in Fig. 3 [10]. The straight lines were calculated by equations (2) and (5), where the value of $\sigma_t$ was calculated by equation (7) [16] by using the value of Weibull modulus, m, of 10.

Table 2 Characteristic of the solvents, $\sigma_v^*$, $\sigma_d^*$ and $\Delta T_c$ of 3Y-TZP and $Al_2O_3$ in various quenching media [10]

| | Methyl alcohol | Glycerin | Water |
|---|---|---|---|
| k(W/m·K) | 0.216 | 0.285 | 0.574 |
| $cx10^{-3}$(J/kg K) | 2.51 | 2.39 | 4.20 |
| $\rho x10^3$(kg/m$^3$) | 0.792 | 1.26 | 1.00 |
| $\mu x10^6$(kg/m·sec) | 0.59 | 1500 | 1.79 |
| $Bx10^6$(1/K) | 1700 | 610 | 53 |
| $\sigma_v^*$(3Y-TZP) | 0.167 | 0.035 | 0.189 |
| $\sigma_d^*$(3Y-TZP) | 0.180 | 0.236 | 0.341 |
| $\Delta T_c$(3Y-TZP) | 350 | 475 | 275 |
| $\sigma_v^*(Al_2O_3)$ | 0.017 | 0.003 | 0.020 |
| $\sigma_d^*(Al_2O_3)$ | 0.069 | 0.095 | 0.150 |
| $\Delta T_c(Al_2O_3)$ | 350 | 325 | 200 |

$r_m$ = 2 mm

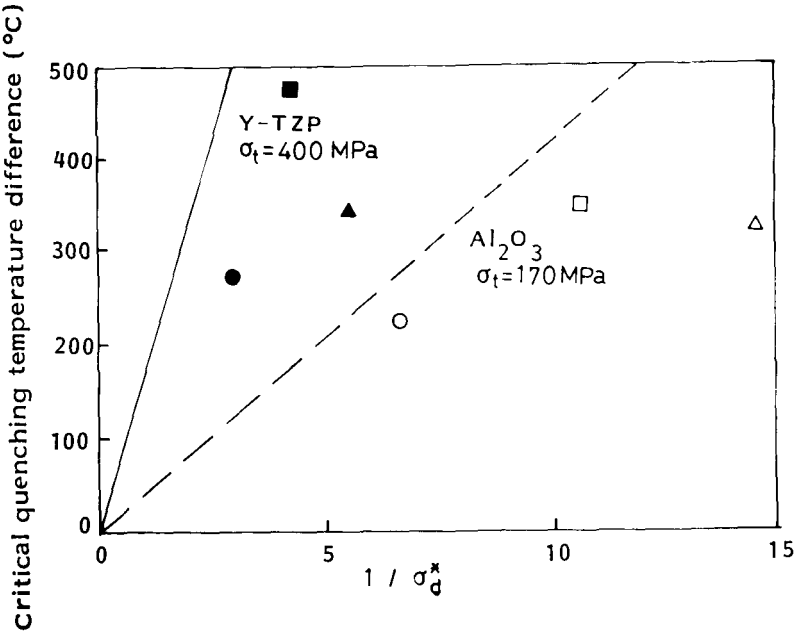


Fig. 3 Relationship between the critical temperature difference and the reciprocal of the nondimentional maximum stress for conductive heat transfer [10]. Quenching media- o:$Al_2O_3$ into water, △ :$Al_2O_3$ into methyl alcohol, □ :$Al_2O_3$ into glycerin, ●:3Y-TZP into water, ▲:3Y-TZP into methyl alcohol, ■ :3Y-TZP into glycerin.

$$\sigma_t / \sigma_{3b} = [1/2(m+1)^2]^{1/m} \quad (7)$$

As seen in Fig. 3, the experimental values of $\Delta T_c$ were significantly smaller than the calculated ones. These results indicated that thermal shock fracture of the samples was not initiated by the thermal stress due to conductive heat transfer, but the convective heat transfer accompanied by boiling of the solvents played an important role for the thermal stress fracture under the present experimental conditions.

$\Delta T_c$ of various zirconia based ceramics, $Al_2O_3$, mullite, SiC and $Si_3N_4$ determined by quenching test into water at $0^oC$ are listed in Table 3 [10] together with 3-point bending strength, $\sigma_{3b}$, of the samples. Since $\sigma_{3b}$ of zirconia ceramics significantly decreased with increasing temperature, the values of $\sigma_{3b}$ both at room temperature and at $300^oC$ were listed in Table 3. From equations (2) and (3), it can be expected that the thermal shock resistance of ceramic materials is improved by increasing the fracture sterngth and decreasing the thermal stress. The relationship between $\Delta T_c$ and $\sigma_{3b}$ at $300^oC$ for zirconia ceramics is shown in Fig. 4 [10]. As expected, $\Delta T_c$ linearly increased with increasing $\sigma_{3b}$, but these plots were divided into two groups. The slope of the straight line for 2Y-TZP, 3Y-TZP and 2Y-TZP/$Al_2O_3$ composites was noticeably smaller than that for other zirconia ceramics.

Since k/rh is positive, equation (8) can be derived from

$$\Delta T_c > 1.451\ \sigma_t(1-\nu)/\alpha E \quad (8)$$

equations (3) and (4). Therefore, the value of $1.451\ \sigma_t(1-\nu)/\alpha E$ can be considered as a parameter for thermal shock resistance. The plot of observed $\Delta T_c$ versus $1.451\ \sigma_t(1-\nu)/\alpha E$ is shown in

Table 3 Bending strength and critical temperature difference of various ceramics quenched into water at 0°C [10]

| Material | $\sigma_{3b}$(MPa) at 25°C | $\sigma_{3b}$(MPa) at 300°C | $\Delta T_c$(°C) |
|---|---|---|---|
| $Al_2O_3$ | 300 | | 225 |
| $Si_3N_4$ | 500 | | 750 |
| SiC | 330 | | 425 |
| Mg-PSZ | 460 | 353 | 300 |
| 6Y-CSZ | 240 | | 200 |
| 3Y-TZP | 900 | 700 | 275 |
| 2Y-TZP | 1300 | 900 | 250 |
| 2Y-TZP/10vol%$Al_2O_3$ | 1720 | 1200 | 250 |
| 2Y-TZP/20vol%$Al_2O_3$ | 2060 | 1300 | 300 |
| 2Y-TZP/40vol%$Al_2O_3$ | 2070 | 1450 | 325 |
| 8Ce-TZP | 600 | 439* | 360 |
| 12Ce-TZP | 425 | 311* | 290 |
| 16Ce-TZP | 160 | 117* | 260 |

* Estimated

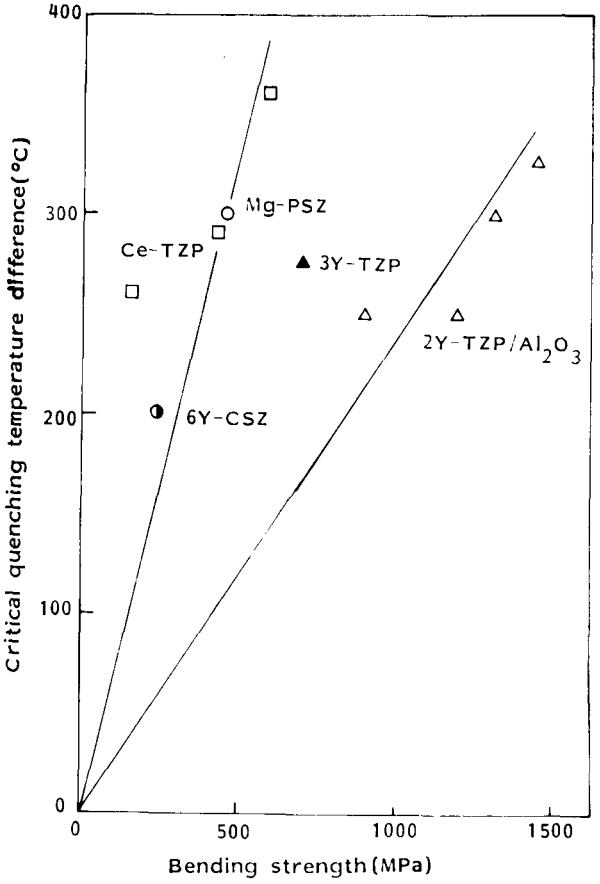


Fig. 4 Relationship between the fracture strength and the critical water quenching temperature difference of 6Y-CSZ, Mg-PSZ, Ce-TZP, 3Y-TZP and 2Y-TZP/$Al_2O_3$ composites [10].

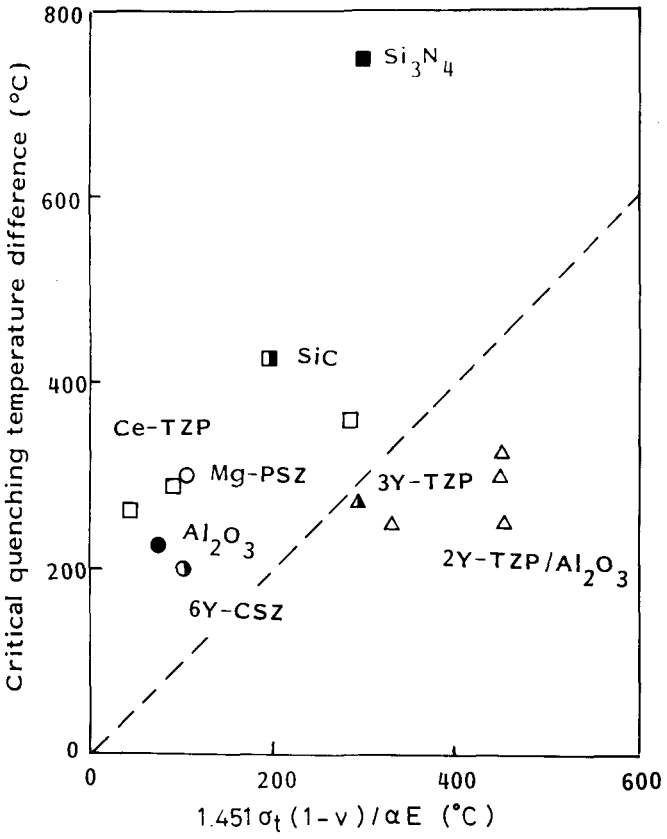


Fig. 5 Relationship between $T_c$ and thermal shock resistance parameter, $1.451\ \sigma_t(1-\nu)/\alpha E$ [10].

Fig. 5 [10]. The slope of the dashed line is 1 which coressponds to the case $h=\infty$. The plots of $\Delta T_c$ in Ce-TZP, Mg-PSZ, 6Y-CSZ, $Al_2O_3$, mullite, SiC and $Si_3N_4$ located above the dashed line as expected by equation (8), but those of Y-TZP based ceramics such as 2Y-TZP, 3Y-TZP and 2Y-TZP/$Al_2O_3$ composites were below the dashed line. These peculiar results indicated that the cracks which cause strength degradation in Y-TZP based ceramics were propagated by the thermal stress lower than the tensile stress calculated by equation (7) using the value of $\sigma_{3b}$.

The heat transfer coefficient, h, calculated by equations (3) and (4) using the results listed in Table 3 for $Al_2O_3$, mullite, SiC, $Si_3N_4$, Mg-PSZ, 6Y-CSZ and Ce-TZP is shown in Fig. 6 as a function of $\Delta T_c$. The values of h shown in Fig. 6 were significantly larger than that calculated for natural convection, $h=1910\ W/m^2 \cdot K$ (log h = 3.28) and increased with increasing $\Delta T_c$. These results indicated that the heat transfer between the sample and solvent were promoted by boiling of the solvent. From the results shown in Fig. 6, it might be possible to assume the value of h as about $10^4\ W/m^2 \cdot K$ when the thermal shock fracture of Y-TZP and Y-TZP/$Al_2O_3$ ocurred under the conditions of $\Delta T_c$ = 250-350°C. Using the value of $h=10^4\ W/m^2 \cdot K$, the thermal fracture stresses of 2Y-TZP, 3Y-TZP, 2Y-TZP/$Al_2O_3$ composites were calculated as 235-285 MPa by equations (3) and (4). These values were significantly smaller than $\sigma_t$=520-1200 MPa determined by equation (7) using the value of $\sigma_{3b}$. These peculiar results indicated that the thermal shock fracture of Y-TZP based ceramics proceeded by the different mechanism with the mechanical fracture.

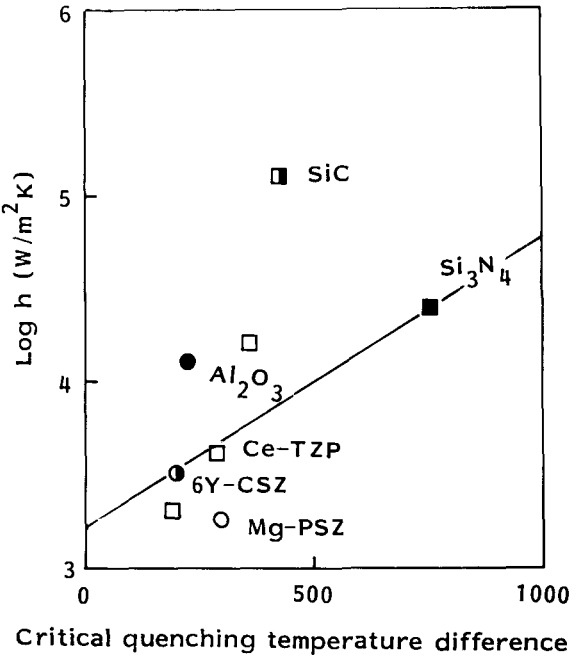


Fig. 6 Calculated values of heat transfer coefficient of various ceramics at critical temperature difference [10].

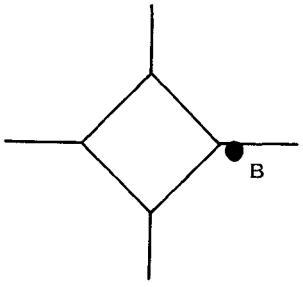


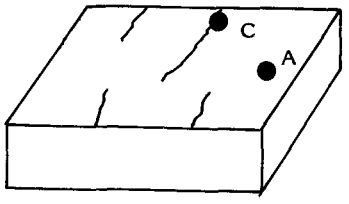


A: Without crack
B: Around crack induced by the Vickers indentation
C: Around crack induced by the thermal stress

Fig. 7 Schmatic diagram illustrating the crack introduced by Vickers indentation and thermal stress and the positions of the laser beam.

The tetragonal to monoclinic phase transformation behavior of Mg-PSZ and 2Y-TZP/40 wt% $Al_2O_3$ ceramics around cracks introduced by both Vickers indentation and by thermal stress was investigated by using Raman microprobe spectroscopy. The Ar-ion laser beam was focussed arounf the crack. The beam position of the Raman microprobe around the cracks is schematically shown in Fig. 7. Raman microprobe spectra of as-polished surface (A), around the crack introduced by Vickers indentation (B) and by thermal stress (C) in Mg-PSZ and 2Y-TZP/40 wt% $Al_2O_3$ are shown in Figs. 8 [17] and 9 [17], respectively. Only the peaks at 148 and 264 $cm^{-1}$ corresponding to the tetragonal bands [18] were observed in the Ramn spectra of as-polished surface of both samples. On the other hand, the monoclinic doublet at 181 and 192 $cm^{-1}$ and additional monoclinic band at 224 $cm^{-1}$ were observed together with the tetragonal bands in the Raman spectra around the indentation cracks of both samples. The amount of the monoclinic phase formed by the Vickers indentation evaluated from the Raman intensity ratio of $(I_m^{181}+I_m^{192})/(I_m^{181}+I_m^{192}+I_t^{148}+I_t^{264})$ [19] were in the order of Mg-PSZ > 2Y-TZP/40 wt% $Al_2O_3$. These results agreed with the facts that Mg-PSZ shows the large transformation zone and excellent fracture toughness about 12 $MPa \cdot m^{1/2}$ [20] and 2Y-TZP/40 wt% $Al_2O_3$ possesses high fracture strength of 2000 MPa, but moderate transformation zone and fracture toughness about 7 $MPa \cdot m^{1/2}$ [6]. The Raman microprobe apectrum around the crack introduced by thermal stress in Mg-PSZ was almost similar to that around the indentation crack. On the other hand, the Raman spectra around the cracks introduced by thermal stress in 2Y-TZP/40 wt% $Al_2O_3$ showed much smaller peaks of the monoclinic phase than those around the Vickers indentation. These results

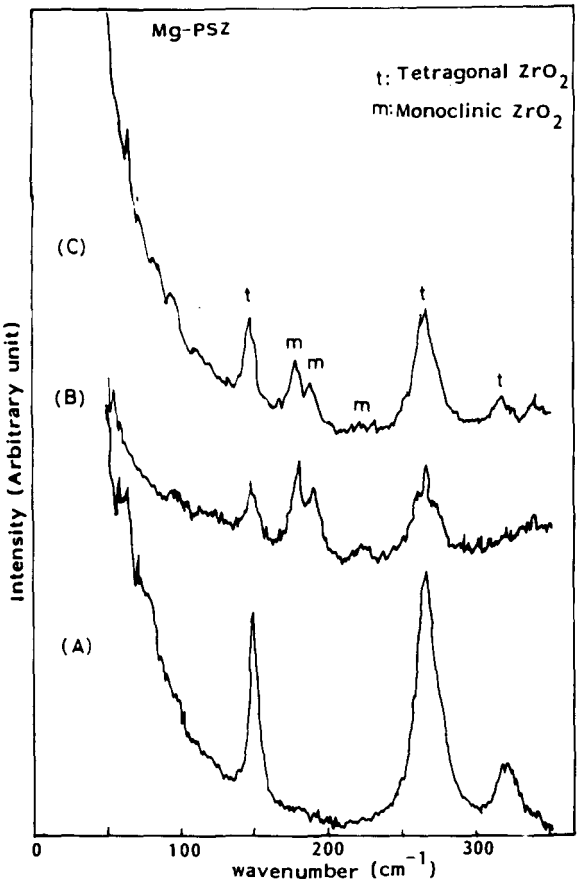


Fig. 8 Raman spectra of Mg-PSZ: (A) As-polished, (B) Around the crack introduced by Vickers indentation, (C) Around the crack introduced by the thermal stress [17].

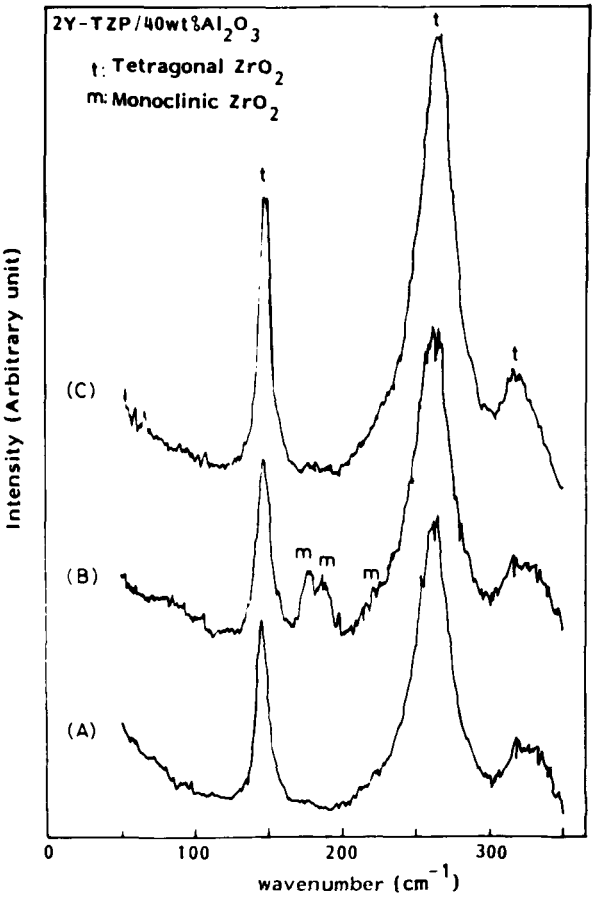


Fig. 9 Raman spectra of 2Y-TZP/40 wt% $Al_2O_3$: (A) As-polished, (B) Around the crack introduced by Vickers indentation, (C) Around the crack introduced by the thermal stress [17].

indicated that the tetragonal to monoclinic phase transformation was caused similarly by both the mechanical stress and thermal stress in Mg-PSZ, but the toughening mechanism by the stress-induced phase transformation did not function well against the thermal stress in Y-TZP based ceramics. Consequently the thermal shock fracture of Y-TZP based ceramics is caused by the thermal stress significantly smaller than the original fracture stress.

Acknowlegement

This work was supported in part by a grant-in-aid for Scientific Research of the Ministry of Education and a grant-in-aid for Developmental Scientific Research of the Ministry of Education.

Reference

1. D.P.H. Hasselman, "Strength Behavior of Polycrystalline Alumina Subjected to Thermal Shock," J. Am. Ceram. Soc., 53 490-495 (1970).

2. J.P. Singh, Y. Tree and, D.P.H. Hasselman, "Effect of Bath and Specimen Temperature on the Thermal Stress Resistance of Brittle Ceramics Subjected to Thermal Quenching, " J. Mater. Sci., 16 2109-2118 (1981).

3. M. Oguma. C.J. Fairbanks and, D.P.H. Hasselman, "Thermal Stress Fracture oof Brittle Ceramics by Conductive Heat Transfer in a Liquid Metal Quenching Medium," J. Am. Ceram. Soc., 69 C87-C88 (1986).

4. D. Lewis, "Comparison of Critical $\Delta T_c$ Values in Thermal Shock with the R Parameter," J. Am. Ceram. Soc., 63 713-714 (1980).

5. K. Tsukuma and M. Shimada, "Hot Isostatic Pressing of $Y_2O_3$ Partially Stabilized Zirconia," Am. Ceram. Soc. Bull.,64 310-313 (1985).

6. K. Tsukuma, K. Ueda, K. Matsushita and, M. Shimada, "Strength and Fracture Toughness of Isostatically Hot-Pressed Composites of $Al_2O_3$ and $Y_2O_3$-Partially-Stabilized $ZrO_2$," J. Am. Ceram. Soc., 68 C4-C5 (1985).

7. M. V. Swain, "The Effect of Decoompoosition on the Thermal Shock Behavior of Mg-CSZ," J. Mater. Sci. Lett.,2 279-282 (1983).

8. T. Sato, T. Fukushima, T. Endo and, M. Shimada, "Thermal Shock Resistance of Yttria-Doped Tetragonal Zirconia Polycrystals: Effect of Solvent in Quenching Test," J. Mater. Sci. Lett.,6 1287-1290 (1987).

9. A.H. Heuer and L.H. Schoenlein, "Thermal Shock Resistance of Mg-PSZ," J. Mater. Sci.,20 3421-3427 (1985).

10. M. Ishitsuka, T. Sato, T. Endo, and M. Shimada, "Thermal Shock Fracture Behavior of $ZrO_2$ Based Ceramics," Thermal Shock Fracture Behavior of $ZrO_2$ Based Ceramics," J. Mater. Sci., in press.

11. M. Anzai, Y. Kimura, H. Fujii, K. Abe and, Y. Kubota, "Thermal Shock Behavior of $Y_2O_3$-Partially Stabilized Zirconia,"Yogyo-Kyokai-Shi, 94 577-582 (1986).

12. M. Ishitsuka, T. Sato, T. Endo and M. Shimada, "Sintering and Mechanical Properties of Yttria-Doped Tetragonal $ZrO_2$ Polycrystal/Mullite Composites," J. Am. Ceram. Soc., 70 C342-C346 (1987).

13. J.P. Singh, J.R. Thomas and D.P.H. Hasselman, "Analysis of Effect of Heat-transfer Variables on Thermal Stress Resistance of Brittle Ceramics Measured by Quenching Experiments," J. Am.

Ceram. Soc.,63 140-144 (1980).

14. H. Hencke, J.R. Thomas, and D.P.H. Hasselman, "Role of Material Properties in the Thermal-Stress Fracture of Brittle Ceramics Subjected to Conductive Heat Transfer," J. Am. Cream. Soc.,67 393-398 (1984).

15. J.P. Holman, Heat Transfer, 3rd. ed., McGraw-Hill, New York (1981).

16. D.G.S. Davis, "The Statistical Approach to Engineering Design in Ceramics," Proc. Brit. Ceram. Soc., 22 429-452 (1973).

17. M. Ishitsuka, T. Sato, T. Endo, M. Shimada and H. Arashi, "Raman Microprobe Spectroscopic Studies on Thermal Shock Fracture of $ZrO_2$ Based Ceramics," J. Mater. Sci. Lett., in press.

18. C.M. Phillippi and K.S. Mazdiyasni, "Infrared and Raman Spectra of Zirconia Polymorphs," J. Am. Ceram. Soc., 54 254-258 (1971).

19. D.R. Clarke and F. Adar, "Measurement of the Crystallographically Transformed Zone Produced by Fracture in Ceramics Containing Tetragonal Zirconia," J. Am. Ceram. Soc., 65 284-288 (1982).

20. D.B. Marshall, "Strength Chracteristics of Tranformation-Toughened Zirconia," J. Am. Ceram. Soc., 69 173-180 (1986).